Journal of Nuclear Materials 407 (2010) 200–204

Contents lists available at ScienceDirect

Journal of Nuclear Materials

journal homepage: www.elsevier.com/locate/jnucmat

Binary effect of He and H on the intra- and inter-granular embrittlement in Fe

Z.X. Tian, W. Xiao, F.R. Wan, W.T. Geng *

School of Materials Science & Engineering, University of Science & Technology Beijing, Beijing 100083, China

ARTICLE INFO

Article history:
Received 26 January 2010
Accepted 17 October 2010

ABSTRACT

Both helium and hydrogen are known to degrade the mechanical performance of reactor materials, but their binary effect has not been well understood. Using *ab initio* density functional theory calculations, we have investigated the He–H interactions both in the bulk and at the grain boundary in bcc Fe. We find an attraction of 0.56 eV between one substitutional He and one interstitial H in the bulk and a repulsion of 0.20 eV at the $\Sigma 3\,(1\,1\,1)\,[1\,\bar{1}\,0]$ grain boundary. The attraction of He and H inside a grain means a reduction of combined embrittling effect in intra-granular fracture and the repulsion at the grain boundary means an enhancement of combined embrittling effect in inter-granular fracture. The interaction of He and H are interpreted with electronic structure analyses.

1. Introduction

Large amounts of helium and hydrogen atoms are produced continuously in structural materials by neutron flux within the reactor [1,2]. The recognition of H embrittlement in metals and alloys dates back to the 19th century, but recently He embrittlement has been attracting more attention in studying the evolution of microstructural damage of nuclear materials [3,4]. At low temperatures He leads to irradiation hardening [5] and shortened fatigue life by acting as an obstacle to the movement of dislocations; at high temperatures it results in significant degradation of the tensile, creep and fatigue properties. Interpretations of experimental information suggest that grain boundaries (GBs) provide fast diffusion paths for He atoms [6], and the He accumulation, both in the bulk and at GBs, has major consequences for structural integrity of first-wall materials.

As for the binary effect of the H and He, investigations have been scarce. Some early studies [7] suggested that irradiation-induced He acted as traps for hydrogen to reduce the diffusivity and permeability. Such a synergistic effect of H and He embrittlement in stainless steels was confirmed by Louthan et al. [8]. In another work, Morgan et al. [9] demonstrated that He enhances the H embrittlement in austenitic stainless steels, and these authors attributed this effect to the reduction of the density of free dislocation, trapping of hydrogen at GBs which make twinning and crack nucleation easier.

More recently, a great many of computer simulations had focused on the positioning of He [10,11], the He–He and He-vacancy interactions [12], and the migration [12,13] of He in bulk environment. An atomistic study demonstrated that both substitutional and interstitial He atoms can be trapped at GBs in bcc Fe and the interstitial He is more strongly bound to the GB core than substitutional He.

The fracture mode of materials induced by impurities can be determined by Rice–Wang thermodynamic theory [14]. This theory describes the mechanism of impurity-induced embrittlement by the competition between dislocation crack blunting and brittle boundary separation. The potency of a segregation impurity in reducing the Griffith energy of a brittle boundary separation is a linear function of the difference in binding energies for that impurity at the GB and the free surface (FS). Based on Rice–Wang model, the first-principles calculations have been carried out in the last 20 years to evaluate not only the embrittling or strengthening effect of the single segregants [15–18], but also of the dual impurity on GB cohesion [19,20]. Full-potential linearized augmented plane wave (FLAPW) calculations show that P has an embrittling effect and B has a significant beneficial effect on Fe $\Sigma 3$ GB cohesion [15]. Using the same method, Geng et al. have investigated the H embrittlement on both the Fe $\Sigma 3\,(1\,1\,1)$ and Ni $\Sigma 5\,(2\,1\,0)$ GB [21], as well as the embrittlement effect of He on the Ni GB [18]. On the other hand, from first-principles calculations, Yamaguchi et al. [22–24] demonstrated that the S atoms tend to aggregate at the Ni $\Sigma 5\,(2\,1\,0)$ GB and the repulsive S–S interactions induce boundary expansion, hence a severe decohesion at the Ni GB.

To date, no research on the combined effect of He and H on the mechanical properties of Fe has been reported. Aiming to reveal the interaction of He and H in Fe and its effect on the ductility of

* Corresponding author.
E-mail address: geng@ustb.edu.cn (W.T. Geng).

0022-3115/$ - see front matter © 2010 Elsevier B.V. All rights reserved.
doi:10.1016/j.jnucmat.2010.10.016

host material, we have carried out a first-principles density functional theory (DFT) investigation.

2. Computational details

The pseudo-potential plane wave code we have employed is the Vienna *Ab initio* Simulation Package (VASP) [25]. The electron–ion interaction was described using projector augmented wave (PAW) method [26], the exchange correlation potential using the generalized gradient approximation (GGA) in the Perdew–Burke–Ernzerhof form [27]. We used the cutoff energy of 480 eV for the plane-wave basis. We have modeled the $\Sigma 3$ (1 1 1) tilt GB of Fe using a supercell illustrated in Fig. 1. The two-dimensional lattice constant for stress-free systems was chosen to be the bulk value for bcc Fe, 2.83 Å, which was also reproduced in our GGA-PBE computation. GB(0) denotes the core of GB. Near the GB, the atomic sites are labeled by number counted from the GB plane. One unit cell contains two identical grains (15 atomic layers each) with one layer in common, which form a tilt GB in between. Based on our previous study [28], the thickness of such a cell is large enough to simulate a bulk-like environment in the center of the grain. In Fig. 1a, there is one atom in one Fe (1 1 1) layer. Note that when one H or He atom is put into GB(0) or GB(2), we are in fact introducing a full monolayer of impurity. This is obviously a very high impurity concentration. Test calculations on a unit cell with a doubled size in the (1 1 1) plane along the $[1\,1\,\bar{2}]$ direction (Fig. 1b) have also been carried out to discuss the effect of impurity concentration. A $(6 \times 6 \times 1)$ k-mesh within Monkhorst–Pack scheme was used. Lattice relaxation was continued until the forces on all the atoms were converged to less than 10^{-3} eV Å^{-1}.

3. Results and discussion

3.1. Interaction of H and He inside the grains

We put both He and H in the unit cell and performed total energy calculations. The H atom moves from the tetrahedral site to the octahedral site upon geometry optimization. Around GB(8), the He–H pair has a combined solution energy of 1.73 eV, in reference to He and H monolayer. Note that this number is 0.56 eV smaller than the summation of that for an individual He and H. We thus arrive at the conclusion that He and H are attractive to each other in bcc Fe. The pairing energy of He–H is −0.56 eV. This strong attraction is due to the decreased electron density around He. It is similar to the case of strong hydrogen trapping at He site in W [29]. The introduction of substitutional He in metals cannot fill up the electron density hole in the interstitial region and the H prefers to reside in an electron-depleted region by reducing the number of its bonding coordination. Under this pulling force, H shift from the tetrahedral site towards the octahedral site. On the free surface, He does not interact with other atoms indeed, the attraction between He and H inside a grain will cancel out their embrittling effect to a certain extent. In addition, the He–H pair impedes movement of the dislocation, leading to hardening and more severe embrittlement in material.

3.2. Binary effect at the Fe GB: high concentration

In Table 1 we list the calculated solution energy E_b of He at various lattice sites near or away from the GB. E_b is defined as:

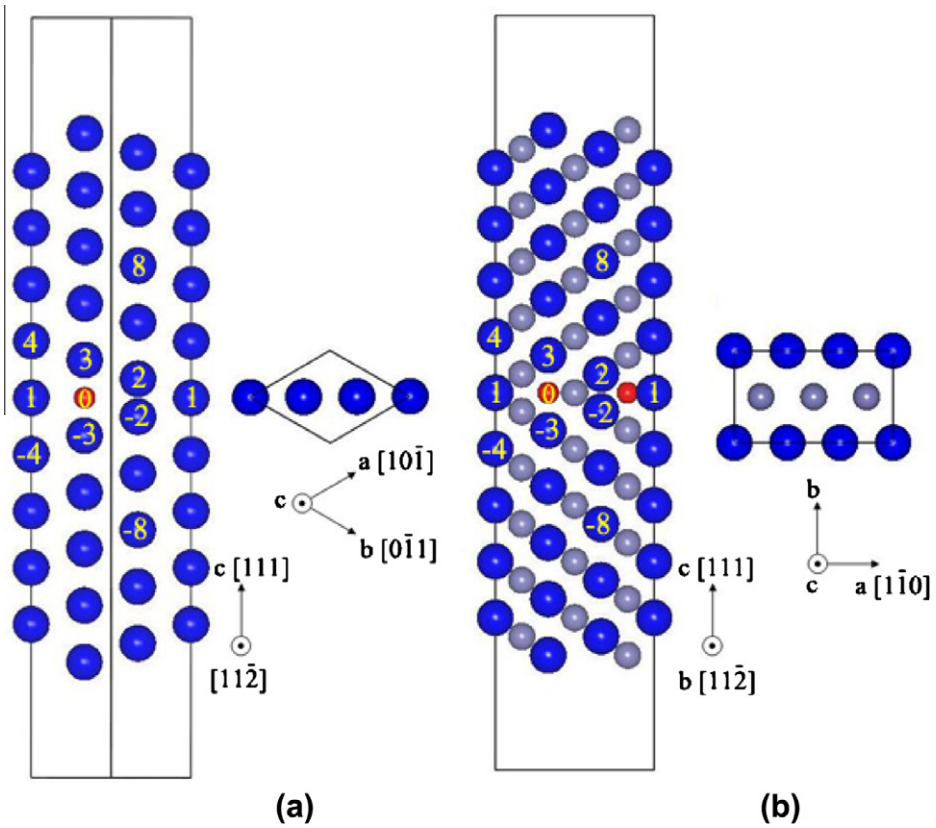

Fig. 1. Side and top views of the computational cell used to model the $\Sigma 3$ (1 1 1) [1 $\bar{1}$ 0] tile grain boundary in bcc Fe. Atoms near the GB are numbered by the atomic layer counted from the GB plane. GB(0) denotes the interstitial site at the GB core. In Panel (b) the cell size doubles that in Panel (a) in the (111) plane, the large dark blue spheres represent atoms in the $(1\,1\,\bar{2})$ plane, and the small light blue spheres represent atoms on $(2\,2\,\bar{4})$ plane. (For interpretation of the references to colour in this figure legend, the reader is referred to the web version of this article.)

Table 1
The calculated solution energies (in eV) of a He atom near or away from the Fe Σ3 (1 1 1) GB. Note that GB(8) is in the center of a grain, and GB(0) is at the grain boundary core. (See Fig. 1a.)

He at	GB(1)	GB(2)	GB(3)	GB(4)	GB(8)	GB(0)
E_b	3.61	2.96	3.45	4.37	4.33	3.0

$$E_b = E(\mathrm{He/GB}) - E(\mathrm{He}) - E(\mathrm{GB}),$$

where, E(He), E(GB) and E(He/GB) represent total energies of He (nearly zero indeed), clean Fe GB and He segregated GB slabs, respectively.

Apparently, all the sites 0, 1, 2 and 3 which are at the GB are much more stable than GB(8) which has a bulk-like environment. This means that He has a strong tendency to segregate to the GB. The driving force underlying this segregation is mainly the extra free volume available at the GB. Hydrogen has already been known to occupy a tetrahedral interstitial site in bcc Fe [30], and this is further confirmed in our calculations. To determine if H atoms segregate to the GB, we evaluated the total energies of two unit cells, one with H residing on tetrahedral interstitial site near GB(8), and the other with H near GB(0). After full geometry optimization, it turns out that the solution energy of H is −2.05 eV around GB(8) and −2.51 eV around GB(0), in reference to H monolayer. This means that H has a potency of 0.46 eV to segregate from inside a grain to the GB. Thus our *ab initio* calculations demonstrated unambiguously that both He and H segregate to the Σ3 GB in Fe.

According to the set up of our supercell, the He–He and H–H distance in neighboring periodical cells is $\sqrt{2}a = 4.00$ Å, appears to be not large enough to assure vanishing He–He and H–H interaction. We have examined the interaction in a He–He pair as well as H–H pair as a function of their separations in a large cubic cell. The results are displayed in Fig. 2. Our DFT calculations show that significant He–He interaction will not go beyond the next-nearest neighbor ($a = 2.83$ Å), although its oscillation extends to a quite large distance. Also, the H–H repelling in bcc Fe is found to decrease rapidly and becomes very weak beyond a separation of 4.0 Å. This means that the computation cell we have adopted is appropriate to study the He–H interaction.

We have performed calculations on the supercells containing one He and one H at the GB. In fact, we are introducing a full monolayer of the impurity onto the GB when one He or H atom is put into GB(2) or GB(0). Obviously it is a very high impurity concentration. We estimate the occupation probability of the impurity using the McLean's equation,

$$C_{GB} = \frac{C_{bulk}\exp(-E_{seg}/k_BT)}{1 + C_{bulk}\exp(-E_{seg}/k_BT)},$$

where E_{seg} is the segregation energy, C_{bulk} is the concentration of the impurities in a bulk material and k_B is the Boltzmann's constant. In fusion reactors, the production of He in ferritic/martensitic steels due to the fusion neutrons amounts to 200–500 appm (atomic parts per million) per year while the H production may arrive at 800–1500 appm per year [31]. In Fig. 3, we present the occupation probability calculated from the McLean's equation for some impurity concentrations in the bulk at various temperatures. With segregation energies of −1.33, −0.72, −1.37, and −0.88 eV for GB(0), GB(1), GB(2), and GB(3), He atoms have a strong tendency to segregate to the GB, and the occupation probability in GB(0) and GB(2) is very close to one for a large temperature span of 273–1173 K. Since the interstitial H has a segregation energy of about −0.46 eV, the occupation probability of the most stable site at the GB will be also very high under 600 K. Thus, our discussion on segregation of one monolayer of He or H at low temperature is meaningful.

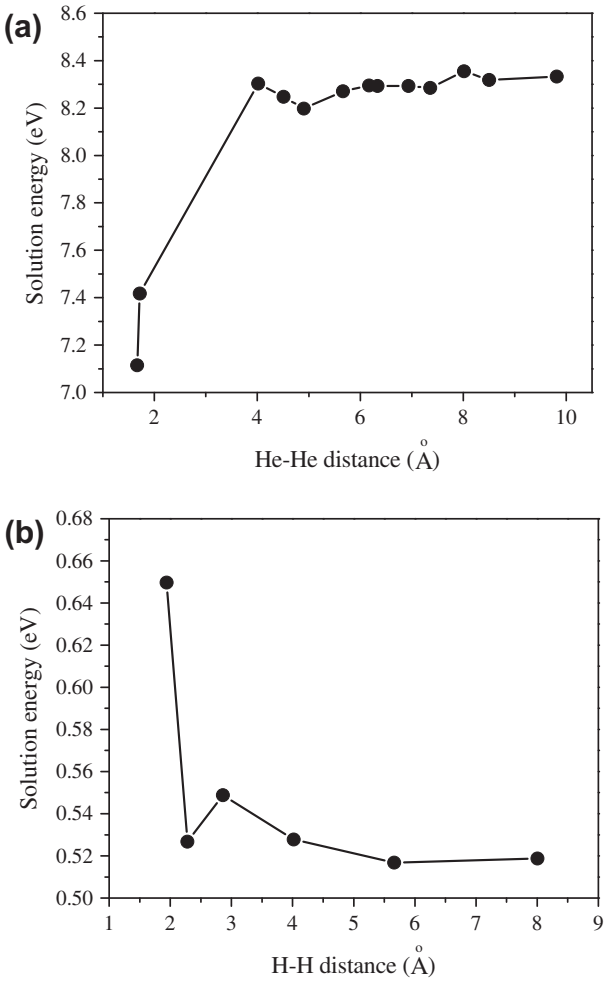

Fig. 2. The calculated solution energy (eV) of a He–He panel (a) or H–H pair panel (b) in a 4 × 4 supercell of bcc Fe as a functions of He–He or H–H separations (Å).

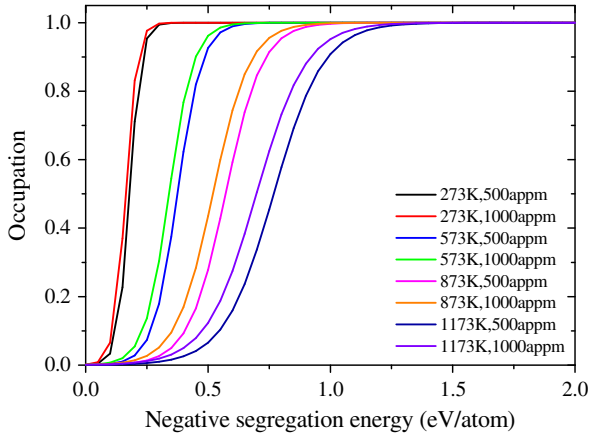

Fig. 3. The calculated occupation probability of the impurities at the GB sites as a function of the segregation energy at different temperatures and bulk concentrations based on the the McLean's equation.

To embark on the study of the interplay between H and He on the Fe GB, one has first to determine the positioning of the H–He pair on the GB. We have calculated the solution energies of the H–He pairs with He locating at different substitutional GB sites (1–4). The results are listed in Table 2. We note that the initial

Table 2
The calculated solution energies (in eV) of the H–He pair with H located at GB(0) and He at different sites near the Fe Σ3 (1 1 1) GB [GB(1) ~ GB(4)].

He at	GB(1)	GB(2)	GB(3)	GB(4)
E_b	1.03	0.64	0.81	1.88

position of H at the GB is different from the setting in the previous work [17]. H is now 0.05 Å off GB(0), which has high symmetry along the $[1\,1\,\bar{2}]$, $[1\,\bar{1}\,0]$ and [1 1 1] directions. After full structural relaxations, we find H is still in the middle of the GB but shifts 0.88 Å along $[1\,1\,\bar{2}]$ direction. Such a relaxation effect was not expected a decade ago, when symmetry constraint was applied due to the limitation in computation resource. When H is located at GB(0), GB(2) is more stable for He than GB(1), GB(3), and GB(4). In the presence of of He, H is pulled close to the $(1\,1\,\bar{2})$ plane. The combined solution energy of the He–H pair [He at GB(2)] at the GB is 0.64 eV, 0.2 eV larger than the summation of that for individual He and H. Therefore, we can draw a conclusion that He at the GB hinders H segregation. The pairing energy of He–H is 0.2 eV. The segregation energy for He to the H/Fe GB [H around GB(0)] is −1.17 eV and it is −0.26 eV for H onto the He/Fe GB [He in GB(2)].

Based on the Rice–Wang model, we calculated the embrittlement effect of the H, He and the H–He pair at Fe Σ3 (1 1 1) GB by first-principles total energy calculations. Table 3 shows the surface and GB segregation energies and the corresponding embrittlement potency of H, He and the H–He pair. Apparently, the H–He pair presents additional strong embrittlement effect. The combined embrittlement energy is larger than the summation of that for individual He and H atoms, i.e. the two can enhance each other's embrittling effect at Fe Σ3 (1 1 1) GB.

To understand the attraction inside the grain and repelling at the GB between He and H, we now resort to the electronic structure analyses of these systems. In Fig. 4 we plot the total valence charge density in the $(1\,1\,\bar{2})$ plane near the Σ3 (1 1 1) $[1\,\bar{1}\,0]$ tilt GB in Fe with and without impurities at their favorable sites. From panel (b) and (c), we see that both substitutional He and interstitial H can increase the charge density in the interstitial region at the GB. For the H/Fe GB, H has two nearest neighbor Fe atoms [on GB(2) and (−2)] with the bond length of 1.78 Å, and these two strong H–Fe bonds induce an increase in charge density in the interstitial region. And for the He/Fe GB, the He atom by occupying GB(2), somewhat like a vacancy, greatly releases the strong internal stress caused by GB(2)–GB(−2) repelling, thereby results in a volume collapse at the GB core and increases charge density in the interstitial region. The helium also has a similar effect on the H–He/Fe GB depicted in panel (d). Not only does it relieve the elastic energy in the complex system, it instantaneously breaks one of the H–Fe bonds too, which provides a driving force for H coming back close to the $(1\,1\,\bar{2})$ plane. Following that, the distance between H and its nearest neighbor Fe atom [GB(2)] reduces to about 1.75 Å, while two Fe atoms [GB(3) and GB(−3)] are found to bind with H at a distance of 1.79 Å. As the bonding capability of H has already been saturated with one H–Fe bond, the excessive H–Fe bonds make the H unstable in this case. Furthermore, owing to a volume decrease induced by helium in the interstitial region, the H on the new site has to subject to more internal stress than it has in the clean GB. Thus, in comparison with the H/Fe GB, the added H–Fe bonds and the re-increased elastic energy associated with the larger internal stress exerting on H lead to a strengthened embrittling effect.

From what have been discussed above, we can safely draw the conclusion that the effect between one substitutional He and one interstitial H at the GB is opposite from that inside the grain. We can attribute this difference to the internal stress presented on the Fe GB cause by the strong repelling of GB(2) and GB(−2). Our calculations demonstrated a GB volume contraction of 4.26 Å^3 associated with He segregation. When both H and He are present at the GB, the volume contraction reduces to 1.51 Å^3. This means that the segregation H to the He-GB introduces a volume expansion of 2.75 Å^3. Note that the GB volume expansion for H segregating to the clean GB is 1.64 Å^3. Apparently, H experiences an increased compression in the presence of He, and hence an additional contribution of elastic energy. In this scenario, one can readily understand that it is the free volume and the internal stress [strong repelling of GB(2)–GB(−2)] that makes the GB different from the bulk, regarding interaction of H and He.

Finally, we note that the shortest distance between He in one cell and H in the adjacent cell is 2.53 Å, seemingly not large enough to minimize the He–H interaction. We have investigated the binary He–H effect in a larger unit cell (see Fig. 1b), in which the distance between H and He in adjacent cells is greater than 4 Å. Results and discussions will be given in the next subsection.

Table 3
The calculated segregation energy of H, He and the pair of H–He on the bcc Fe (1 1 1) surface and the Fe Σ3 (1 1 1) $[1\,\bar{1}\,0]$ GB. The corresponding embrittlement energies are also presented.

	He	H	He–H pair
E_{seg}^{fs}	−4.33	−0.78	−4.57
E_{seg}^{gb}	−1.37	−0.46	−1.09
E_b	2.96	0.32	3.48

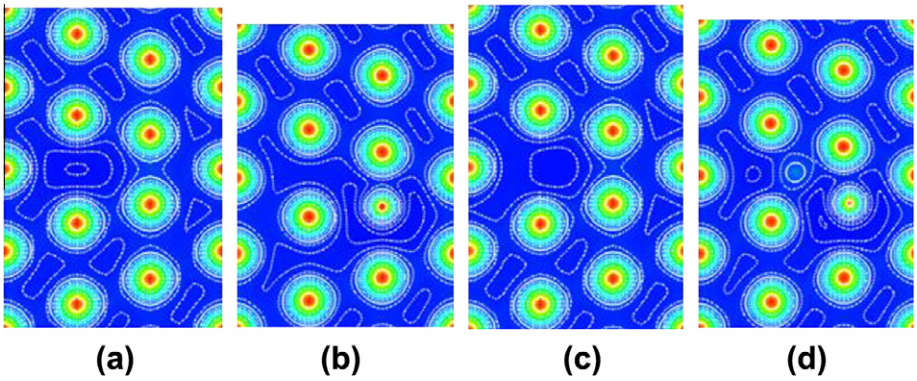

Fig. 4. The calculated total valence charge density for (a) the clean Fe GB, (b) He/Fe GB, (c) H/Fe GB and (d) He–H/Fe GB. Lines start from 0.01 e/a.u.^{3} and increase successively by a factor of $10^{1/5}$.

3.3. Binary effect at the Fe GB: low concentration

To make the discussion more complete, we have also checked the interaction of the H–He pair in a low concentration case with an expanded unit cell, as shown in Fig. 1b.

We put He at GB(2) and H at GB(0), 0.05 Å off along the $[1\,1\,\bar{2}]$ direction on the $(1\,1\,\bar{2})$ plane. The concentration for each impurity at the GB is 50%. The calculated combined solution energy of the H–He pair is 1.0 eV, 0.24 eV more than the addition of individual He and H. Apparently, the repulsive effect is nearly the same as what we obtained in the high impurity concentration case. This means that the interaction of H and He in adjacent cells is negligible, and thus the computation cell shown in Fig. 1a is appropriate to discuss the binary effect of the H–He pair at the GB.

Furthermore, we checked the case for both He and H being located at GB(0) [there are two GB(0) sites in Fig. 1b]. The combined solution energy is found to be 0.545 eV, smaller than that the GB(2)–GB(0) pair in the $(1\,1\,\bar{2})$ plane. The calculated solution energy of a GB(0) He (H) is 3.02 eV (−2.495 eV). This means the repelling between the H and He located at neighboring GB(0) sites is 0.02 eV. The optimized H–He distance is 3.16 Å. We note that the distance between H and He in adjacent cells is 4.17 Å, thus those interactions are expected to be even smaller.

Our numerical results show that neither H nor He will cause a remarkable distortion of the atomic alignment at the GB. The volume expansions induced by He and H at GB(0) are about 2.72 $Å^3$ and 1.88 $Å^3$, respectively, in reference to the relaxed clean Fe GB. When both H and He are present at the interstitial site of the GB, the volume expansion increases to 4.38 $Å^3$. Thus, the binary H–He effect reflected on the volume change is −0.22 $Å^3$. The small volume change associated with segregation makes the H–Fe and He–Fe bonding unaffected by each other.

4. Conclusion

To summarize, we have carried out a detailed study on the interaction of the He–H pair in iron. In the bulk, the substitutional He acts as a strong trap for the interstitial H nearby and makes H shift from the tetrahedral- to the octahedral–interstitial site due to a decreased electron density surrounding it. Thus they remedy each other's embrittling effect in intra-granular fracture. At the grain boundary, the segregated He, relieves the internal stress, reduces significantly the volume of the GB core, and leads to a charge density increase in this region. As a consequence, the stability of the H nearby is lowered. Therefore, He and H facilitate each other's embrittling behavior in the inter-granular fracture of iron.

Acknowledgments

This work was supported by the NSFC (Grant No. 50971029) and MOST (Grant No. 2009GB109004) of China. The calculations were performed on the Quantum Materials Simulator of USTB.

References

[1] R. Sugano, K. Morishita, H. Iwakiri, N. Yoshida, J. Nucl. Mater. 307 (2002) 941.
[2] B. Stahl, E. Kankeleit, G. Walter, Nucl. Instrum. Methods Phys. Res. Sect. B-Beam Interact. Mater. Atoms 211 (2003) 227.
[3] E.E. Bloom, J. Nucl. Mater. 258–263 (1998) 7.
[4] H. Ullmaier, Nucl. Fusion 24 (1984) 1039.
[5] R.L. Klueh, D.J. Alexander, J. Nucl. Mater. 218 (1995) 151.
[6] H. Trinkaus, B.N. Singh, J. Nucl. Mater. 323 (2003) 229.
[7] K. Fukushima, K. Ebisawa, S. Nakahigashi, M. Iimura, M. Terasawa, J. Nucl. Mater. 127 (1985) 109.
[8] M.R. Louthan, N.C. Iyer, M.J. Morgan, Mater. Charact. 43 (1999) 179.
[9] M.J. Morgan, M.H. Tosten, in: A.W. Thompson, N.R. Moody (Eds.), Hydrogen Effects In Materials, TMS, 1996, pp. 873.
[10] R.J. Kurtz, H.L. Heinisch, J. Nucl. Mater. 329–333 (2004) 1199.
[11] X.T. Zu, L. Yang, F. Gao, S.M. Peng, H. Heinisch, X.G. Long, R.J. Kurtz, Phys. Rev. B 80 (2009) 054104.
[12] C.C. Fu, F. Willaime, Phys. Rev. B 72 (2005) 064117.
[13] F. Gao, H. Heinisch, R.J. Kurtz, J. Nucl. Mater. 351 (2006) 133.
[14] J.R. Rice, J.S. Wang, Mater. Sci. Eng. A 107 (1989) 23.
[15] R. Wu, A.J. Freeman, G.B. Olson, Science 265 (1994) 376.
[16] W.T. Geng, A.J. Freeman, R. Wu, G.B. Olson, Phys. Rev. B 62 (2000) 6208.
[17] L. Zhong, R. Wu, A.J. Freeman, G.B. Olson, Phys. Rev. B 62 (2000) 13938.
[18] R.W. Smith, W.T. Geng, C.B. Geller, R. Wu, A.J. Freeman, Scripta Mater. 43 (2000) 957.
[19] L. Zhong, R. Wu, A.J. Freeman, G.B. Olson, Phys. Rev. B 55 (1997) 11133.
[20] W.T. Geng, A.J. Freeman, G.B. Olson, Solid State Commun. 119 (2001) 585.
[21] W.T. Geng, A.J. Freeman, G.B. Olson, Y. Tateyama, T. Ohno, Mater. Trans. 46 (2005) 756; and references therein.
[22] M. Yamaguchi, M. Shiga, H. Kaburaki, Science 307 (2005) 393.
[23] W.T. Geng, J.S. Wang, G.B. Olson, Science 309 (2005) 1677c.
[24] M. Yamaguchi, M. Shiga, H. Kaburaki, Science 309 (2005) 1677d.
[25] G. Kresse, J. Furthmuller, Phys. Rev. B 54 (1996) 11169.
[26] G. Kresse, D. Joubert, Phys. Rev. B 59 (1999) 1758.
[27] J.P. Perdew, K. Burke, M. Ernzerhof, Phys. Rev. Lett. 77 (1996) 3865.
[28] W.T. Geng, A.J. Freeman, G.B. Olson, Phys. Rev. B 63 (2001) 165415.
[29] B. Jiang, F.R. Wan, W.T. Geng, Phys. Rev. B 81 (2010) 134112.
[30] D.E. Jiang, E.A. Carter, Phys. Rev. B 70 (2004) 064102.
[31] R. Schaublin, J. Henry, Y. Dai, C. R. Phys. 9 (2008) 389.